JOURNAL OF SOLID STATE CHEMISTRY 37, 271–278 (1981)

Chemical Diffusion in Intermediate Phases in the Lithium–Silicon System

C. JOHN WEN* AND ROBERT A. HUGGINS

Department of Materials Science and Engineering, Stanford University, Stanford, California 94305

Received June 13, 1980; in final form September 3, 1980

The equilibrium coulometric titration curve shows four intermediate phases in the Li–Si system at 415°C. The nominal compositions for these phases are $Li_{12}Si_7$, Li_7Si_3, $Li_{13}Si_4$, and $Li_{22}Si_5$, respectively. They all have quite narrow ranges of homogeneity. The compositional variations of the chemical diffusion coefficients within the various intermediate phases are similar to each other and closely resemble those of the thermodynamic enhancement factor for each phase. The chemical diffusion coefficients across all four intermediate phases are essentially of the same order, about 6.0×10^{-5} cm²/sec at 415°C.

Introduction

There is much current interest in lithium-based battery systems with molten salt electrolytes. These batteries are generally operated at temperatures of 400–450°C. Present versions employ either lithium–aluminum (*1, 2*) or lithium–silicon (*3–5*) alloys as active constituents in their negative electrodes.

The work reported here is part of a series of investigations of the thermodynamic and kinetic properties of a number of lithium alloy systems which might be considered for use as negative electrode reactants in lithium-based batteries. The lithium chemical potential and its compositional dependence determine the potential and the capacity of electrode reactants. The fundamental parameter related to their kinetic behavior is the chemical diffusion coefficient, which controls the rate of compositional equilibration within the solid constituents of the electrode structure. This paper reports experimental results on the compositional variations of the emf, the thermodynamic enhancement factor (TEF), the chemical diffusion coefficient, and the lithium self-diffusion coefficient across the four intermediate phases in the Li–Si system.

Only two intermediate phases, with nominal compositions Li_2Si and Li_4Si, are indicated in the standard Li–Si phase diagram (*6, 7*). The crystal structures of the phases Li_2Si (*8*) and Li_4Si (*9*) were determined, but their detailed X-ray diffraction patterns were not given. Li–Si alloys with various nominal compositions such as $Li_{13}Si_7$ (*9*), $Li_{13}Si_4$ (*10*), $Li_{10}Si_3$ (*11*), Li_7Si_2 (*12*) $Li_{15}Si_4$ (*13, 14*), and $Li_{22}Si_5$ (*15, 16*) have also been reported in the literature. Structural work (*15, 16*) indicates, however, that $Li_{22}Si_5$ (isostructural with $Li_{22}Pb_5$) rather than

* Presently at Shell Development Co., Houston, Tex.

0022-4596/81/060271-08$02.00/0

$Li_{15}Si_4$ or Li_4Si is actually the most Li-rich phase of the Li–Si system. The crystal structure of $Li_{13}Si_4$, earlier reported as Li_7Si_2 (*12*), was redetermined by Frank *et al.* (*10*). Very recently, a careful study by von Schnering *et al.* (*17, 18*) also indicated that orthorhombic $Li_{12}Si_7$ rather than $Li_{13}Si_7$, as reported in the literature, is the most Si-rich phase. Furthermore, the next phase is the violet $Li_{14}Si_6$ (*18*) or $Li_{5-x}Si_2$, where x is nearly 0.33. This phase is isostructural with Li_5Sn_2 (*19*), and can be nominally represented by Li_7Si_3. Thus these structural results indicate phases with nominal compositions $Li_{12}Si_7$, Li_7Si_3, $Li_{13}Si_4$, and $Li_{22}Si_5$, or y = 1.71, 2.33, 3.25, and 4.4, in the formula Li_ySi.

Investigations of nonequilibrium electrochemical discharge of Li–Si alloys (*20, 21*) and dynamic charging of silicon (*4*) have shown four intermediate phases in the Li–Si system at 415°C. McCoy and Lai (*20, 21*) suggested that the four intermediate phases are Li_2Si, $Li_{14}Si_5$, $Li_{41}Si_{10}$, and Li_5Si, i.e., y = 2.0, 2.8, 4.1, and 5.0. On the other hand, Sharma and Seefurth (*4*) concluded that they have the nominal compositions Li_2Si, $Li_{21}Si_8$, $Li_{15}Si_4$, and $Li_{22}Si_5$, corresponding to values of y = 2.0, 2.625, 3.75, and 4.4. However, recently reported equilibrium electrochemical experiments (*18*) indicated that the first two phases appear at about y = 1.7 and 2.33.

The equilibrium electrochemical coulometric titration technique was used in this study in the hope of resolving this disagreement regarding the compositions of the intermediate phases in the Li–Si system. This involves the imposition of precise compositional changes in solid samples by passing known amounts of charge through an appropriate electrochemical cell in which they are used as electrodes, followed by equilibration and the evaluation of the resultant changes in lithium chemical potential by means of potential measurements. In addition, X-ray diffraction analysis was undertaken to help corroborate the existence and formulas of these intermediate phases (*22*).

The self-diffusion coefficient of lithium in silicon has been measured by a number of investigators using various experimental techniques (*23–29*) and has a mean value of about 3.3×10^{-8} cm²/sec at 415°C. No comparable data are available for any of the intermediate phases. Furthermore, proper understanding of the processes occurring when Li–Si alloys are employed as active materials in the negative electrode in high-performance lithium-based batteries requires a knowledge of the chemical diffusion coefficient (which is relevant to diffusion in the presence of a concentration gradient) as a function of composition in these phases. No such information appears to be available in the literature.

Experimental Procedures

The coulometric titrations, emf, and chemical diffusion measurements were all made using the following three-electrode type of galvanic cell:

$$\text{Al,“LiAl”(s)}|\text{LiCl–KCl(eut.)}|\text{Li}_y\text{Si(s)}, \quad \text{(I)}$$

where Li_ySi is the Li–Si alloy under investigation, and LiCl–KCl (eut.) is the eutectic molten-salt electrolyte. Al, “LiAl” represents both the reference and counter electrodes, which were composed of a two-phase Li–Al alloy mixture consisting of the saturated solid solution of lithium in aluminum and the intermediate phase “LiAl,” with an overall composition of 40 a/o Li. Similar experimental setups and procedures have been described elsewhere (*22, 30–34*), and thus will not be repeated here.

Semiconductor grade p-type silicon wafers (doped with boron) and Li–Si alloys were both used as starting materials for the coulometric titration experiments. Molybdenum sheets were employed as the electri-

cal leads. The Li–Si alloys used in this study were prepared by a fusion technique inside a helium-filled glovebox in a manner similar to that described previously (*4*). Lithium metal (99.9%), obtained from Foote Mineral, was first melted in a nickel crucible at about 325°C. After adding the appropriate amount of silicon powder (99.99%), purchased from Alfa, Ventron Corp., the temperature was slowly raised to 750°C and maintained at that value for approximately 20 to 30 min. The alloy was cooled to 450°C and annealed for another 18 hr. After annealing, it was slowly cooled to room temperature. The resultant alloys were powdered and sieved through a 150-mesh screen. These powders were cold pressed into pellets of 3/8 in diameter at a pressure of 9×10^4 psi under a helium atmosphere.

The chemical diffusion coefficient was evaluated from the long-time solution of the diffusion equations relevant to a potentiostatic step experiment, as described elsewhere (*32, 34*).

Results

Figure 1 shows the equilibrium open-circuit voltage in the Li–Si system as a function of composition, as determined by use of the coulometic titration technique. Up to the composition of 83 a/o Li, five voltage plateaus were observed. At 415°C, the constant-emf values of the five two-phase regions are 332, 288, 158, 44, and 2 mV, relative to pure liquid lithium, in order of increasing lithium content. The corresponding lithium activity values at that temperature are 3.70×10^{-3}, 7.77×10^{-3}, 6.96×10^{-2}, 0.476, and 0.967, respectively. These results are in good agreement with those previously reported in the literature (*4, 20, 21*).

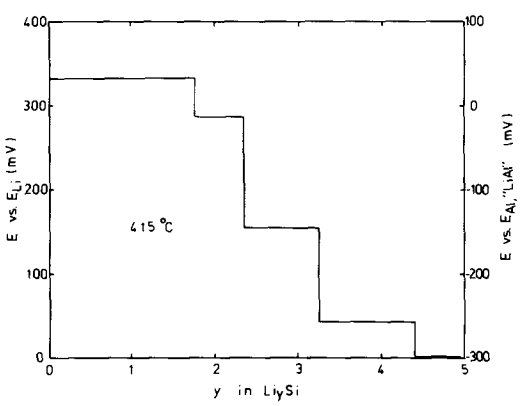

FIG. 1. Coulometric titration curve for the lithium–silicon system at 415°C.

Although no particular effort was made to accurately determine the solid solubility of lithium in silicon, the coulometric titration experiment indicated that it is less than 0.36 a/o Li at 415°C. Figure 1 also shows that these experiments, performed by electrochemically incorporating lithium into a silicon wafer, indicated the presence of four intermediate phases in the Li–Si system. The approximate compositions of these four phases, expressed as y in Li_ySi, were found to be 1.731, 2.367, 3.317, and 4.25, respectively. Using a Li–Si alloy with an overall composition of 72.2 a/o Li as the starting material, the component ratios of the two Li-rich phases were redetermined and found to be 3.237 and 4.41, respectively. These results indicate that the nominal compositions for these four intermediate phases are $Li_{12}Si_7$, Li_7Si_3, $Li_{13}Si_4$, and $Li_{22}Si_5$. As shown in Fig. 1, all the intermediate phases in the Li–Si system have quite narrow ranges of stoichiometry.

The standard Gibbs free energy of formation for the phase Li_aSi_b, $\Delta G_f(Li_aSi_b)$, according to the reaction

$$a\ \mathrm{Li(l)} + b\ \mathrm{Si(l)} \rightleftharpoons \mathrm{Li}_a\mathrm{Si}_b\mathrm{(s)} \qquad \text{(II)}$$

can be determined by graphical evaluation of the area under the coulometric titration curve (E versus y)

$$\Delta G_f^\circ(\mathrm{Li}_a\mathrm{Si}_b) = -bF \int_0^y E\,dy, \qquad (1)$$

where y is the atomic ratio of lithium to silicon. At the temperature of 415°C, the values of the standard Gibbs free energy of formation of the four intermediate phases, assumed to be nominally $Li_{12}Si_7$, Li_7Si_3, $Li_{13}Si_4$, and $Li_{22}Si_5$, are −384, −216, −344, and −445 kJ/mole, respectively.

Phase $Li_{12}Si_7$

The compositional variations of the open-circuit voltage relative to pure lithium and the thermodynamic enhancement factor in the most Si-rich phase $Li_{12}Si_7$ at 415°C are shown in Fig. 2. The coulometric titration curve was slightly shifted so that the inflection point occurs at the nominal stoichiometric composition $Li_{12}Si_7$. This adjustment was made on the basis of a simple defect model (*35*) in which the small deviations from the ideal stoichiometry are expressed as being due to the presence of lithium vacancies and interstitial lithium atoms as the predominant point defects for the Li-poor and Li-rich compositions, respectively. Although this defect model should not be considered valid without further experimental evidence, the data on the emf versus the change in composition, not the absolute composition, are quite precise.

At 415°C, the emf of the phase $Li_{12}Si_7$ lies between 332 and 288 mV with respect to pure liquid lithium. The thermodynamic enhancement factor was calculated from the local slope, $dE/d\delta$, of the coulometric titration curve using the expression

$$\frac{d \ln a_{Li}}{d \ln(a + \delta)} = -\frac{F}{RT}(a + \delta)\frac{dE}{d\delta} \simeq -\frac{aF^2 n_{Si}\Delta E}{bRTQ}, \quad (2)$$

where a_{Li}, F, R, T, Q, n_{Si}, and ΔE are the lithium activity, the Faraday constant, the gas constant, the absolute temperature, the total charge accumulated after each voltage step, the number of gram-atoms of silicon, and the applied voltage step, respectively. In the above expression, a and b are the stoichiometric numbers of the lithium and silicon atoms in the Li–Si phase Li_aSi_b. Within the stability range of $Li_{12}Si_7$, the thermodynamic enhancement factor varies from 122 to 160, with a maximum at the nominal stoichiometric composition.

The mass transport properties within the phase $Li_{12}Si_7$ are presented in Fig. 3. The compositional dependence of the chemical diffusion coefficient is similar to that of the

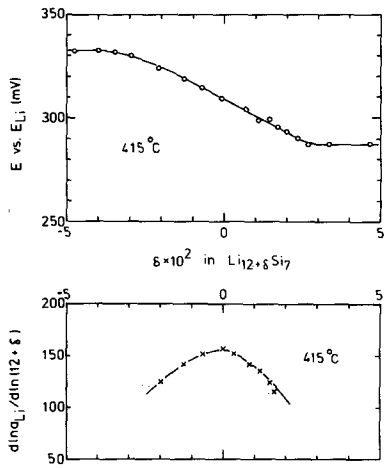

FIG. 2. Thermodynamic properties of the phase $Li_{12}Si_7$.

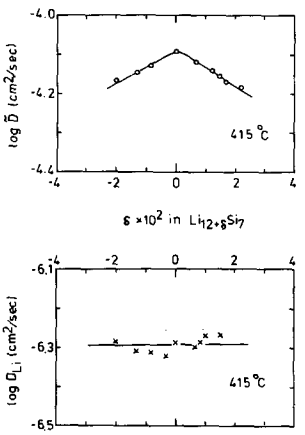

FIG. 3. Transport properties of the phase $Li_{12}Si_7$.

thermodynamic enhancement factor. The chemical diffusion coefficient varies with composition from 6.60×10^{-5} to 8.13×10^{-5} cm²/sec, showing a maximum at the nominal stoichiometric composition. Using these data on the chemical diffusion coefficient and the thermodynamic enhancement factor, the lithium self-diffusion coefficient was determined as a function of composition according to the following equation:

$$\tilde{D} = D_{\mathrm{Li}} \left[\frac{d \ln a_{\mathrm{Li}}}{d \ln (a + \delta)} \right], \qquad (3)$$

with the assumption that the self-diffusion coefficient of the lithium atoms is much higher than that of the silicon atoms. In contrast to the chemical diffusion coefficient, the lithium self-diffusion coefficient in the phase $Li_{12}Si_7$ is essentially composition independent, with an average value of 5.08×10^{-7} cm²/sec at 415°C.

Phase Li_7Si_3

The phase Li_7Si_3 is stable between 288 and 158 mV relative to pure liquid lithium at 415°C. In Fig. 4, the coulometric titration curve shows that the experimental results obtained by electrochemically incorporating lithium into the sample electrode are in accordance with those determined by removing lithium. The calculated thermodynamic enhancement factor in this phase is shown at the bottom of Fig. 4. It changes with composition from 87 to 111, having a maximum value at or near the nominal stoichiometric composition.

Figure 5 shows the compositional dependence of the chemical diffusion coefficient and the lithium self-diffusion coefficient across the phase Li_7Si_3. As more lithium is added, the chemical diffusion coefficient first increases, with the maximum value at the nominal stoichiometric composition. The chemical diffusion coefficient varies with composition from 4.16×10^{-5} to 5.46×10^{-5} cm²/sec at 415°C but the lithium self-diffusion coefficient remains constant within the phase stability range, with a mean value of 4.80×10^{-7} cm²/sec.

Phase $Li_{13}Si_4$

The thermodynamic data for the phase $Li_{13}Si_4$ are presented in Fig. 6. At 415°C, the open-circuit voltage lies between 157 and 44 mV relative to pure lithium. The

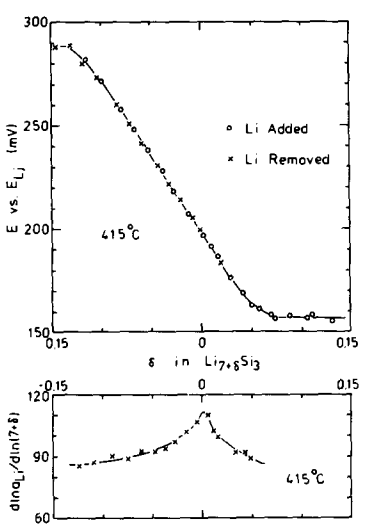

FIG. 4. Thermodynamic properties of the phase Li_7Si_3.

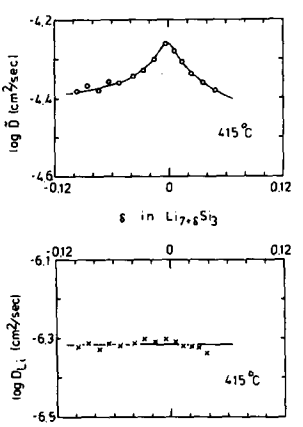

FIG. 5. Transport properties of the phase Li_7Si_3.

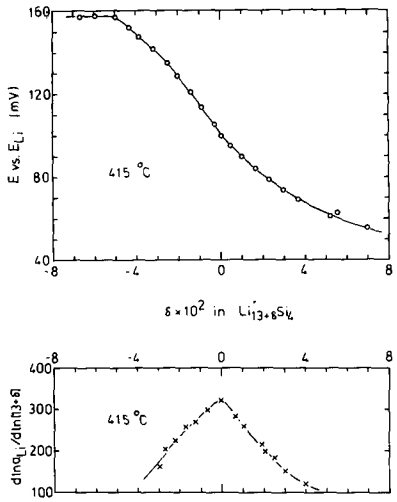

FIG. 6. Thermodynamic properties of the phase $Li_{13}Si_4$.

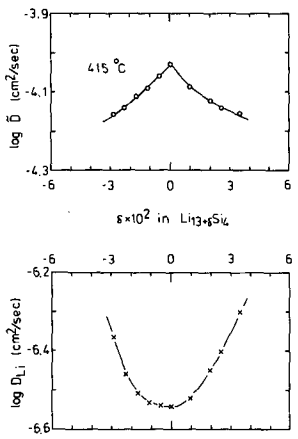

FIG. 7. Transport properties of the phase $Li_{13}Si_4$.

thermodynamic enhancement factor, ranging from 120 to 325, is shown to have a maximum at the nominal stoichiometric composition.

At high lithium activities, a slow voltage drift with time was observed. The total charge, Q, used to calculate the change in composition for each voltage step was the arithmetic mean of charge and discharge. Alternatively, the necessary corrections for Q due to the loss of lithium during potentiostatic titration were made by measuring the residual current in each voltage step. The results were always compared with the theoretical values calculated from the relation $Q = \pi^2 I_0/8k$, where I_0 and k were the extrapolated intercept at $t = 0$ and the slope of a linear plot of current versus time on a semilogarithmic scale, as described previously (*32, 34*).

The chemical diffusion coefficient and lithium self-diffusion coefficient within the phase $Li_{13}Si_4$ are given as functions of composition in Fig. 7. The compositional variation of the chemical diffusion coefficient across this phase is similar to that of the thermodynamic enhancement factor. The chemical diffusion coefficient varies from 7.00×10^{-5} to 9.33×10^{-5} cm²/sec at 415°C and has a maximum at the ideal stoichiometry. The values of the self-diffusion coefficient of lithium in $Li_{13}Si_4$ also change with composition from 2.88×10^{-5} to 5.01×10^{-5} cm²/sec, but show a minimum rather than a maximum near the nominal stoichiometric composition.

Phase $Li_{22}Si_5$

Figure 8 shows the thermodynamic prop-

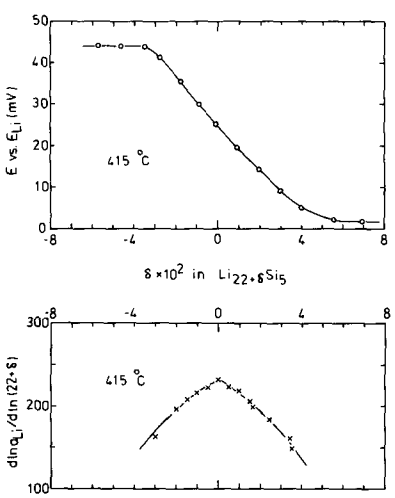

FIG. 8. Thermodynamic properties of the phase $Li_{22}Si_5$.

erties of the most Li-rich intermediate phase $Li_{22}Si_5$ in the Li–Si system. At 415°C, this phase is stable between 44 and 2 mV relative to pure lithium. The emf versus composition data for the phase $Li_{22}S_5$ were determined in the same manner as described above for the phase $Li_{13}Si_4$. The coulometric tritration curve shows an inflection point at the nominal stoichiometric composition so that the thermodynamic enhancement factor, varying from 147 to 232, has a maximum at that composition.

As shown in Fig. 9, the compositional dependence of the chemical diffusion coefficient in the phase $Li_{22}Si_5$ is significantly influenced by the thermodynamic enhancement factor. The chemical diffusion coefficient across this phase shows a maximum value at the nominal stoichiometric composition. While the chemical diffusion coefficient is strongly dependent upon the composition, the lithium self-diffusion coefficient remains essentially constant within the phase stability range, with a mean value of 3.16×10^{-7} cm^2/sec.

Discussion

As shown in the previous sections, the compositional variations of the chemical diffusion coefficients within the various intermediate phases in the Li–Si system are similar to each other and closely resemble those of their thermodynamic enhancement factors. The chemical diffusion coefficients across the four phases are essentially of the same magnitude, about 6.0×10^{-5} cm^2/sec at 415°C. These results can be attributed to the fact that the lithium self-diffusion coefficients and the thermodynamic enhancement factors (TEF) are of the same order of magnitude, as shown in Table I.

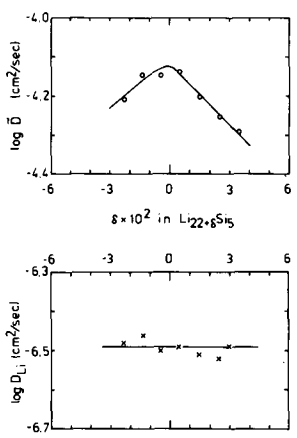

FIG. 9. Transport properties of the phase $Li_{22}Si_5$.

The data reported in the literature on the lithium self-diffusion coefficient in silicon (*23–29*) are also included in Table I for comparison. It is one order of magnitude lower than those in the intermediate phases, as illustrated in column 4. Only limited information is available concerning the thermodynamics of the Li–Si system. At 415°C the solid solubility of lithium in silicon is estimated to be about 10 ppm, using the available data in the literature (*36, 37*). Since the terminal solubility of lithium in silicon is so low, it is not unreasonable to assume that the thermodynamic enhancement factor is close to unity. Under these circumstances, the chemical diffusion coefficient in the dilute solid solution of lithium in silicon is approximately equal to the self-diffusion coefficient of lithium in silicon, about 3.3×10^{-8} cm^2/sec at 415°C. This value is nearly three orders of magnitude lower than the chemical diffusion coefficients in the various intermediate phases at the same temperature.

TABLE I

THERMODYNAMIC AND KINETIC DATA FOR VARIOUS INTERMEDIATE PHASES IN THE Li–Si SYSTEM

Phase	TEF	$\tilde{D}$ (cm^2/sec)	D_{Li} (cm^2/sec)
Si			$1.67–6.56 \times 10^{-8}$
$Li_{12}Si_7$	122–160	$6.60–8.13 \times 10^{-5}$	$4.85–5.44 \times 10^{-7}$
Li_7Si_3	87–111	$4.16–5.46 \times 10^{-5}$	$4.16–4.96 \times 10^{-7}$
$Li_{13}Si_4$	120–325	$7.00–9.33 \times 10^{-5}$	$2.88–5.01 \times 10^{-7}$
$Li_{22}Si_5$	147–232	$5.13–7.24 \times 10^{-5}$	$2.99–3.45 \times 10^{-7}$

We feel that the compositions of the intermediate phases in the Li–Si system at 415°C have now been clarified, as the data obtained in this work correspond quite well with the new structural work, as well as with the other recent equilibrium electrochemical measurements. The disparate results reported by some earlier investigators using electrochemical techniques may be due to two factors. One is their use of dynamic (current flowing) measurements, whereas the results reported here were obtained after equilibration under open circuit conditions. The second is that it is known that electronic leakage occurs in molten-chloride-electrolyte melts at high lithium activities, and this could easily lead to imprecision in the evaluation of composition changes.

Acknowledgments

This work was sponsored by the U.S. Department of Energy under Contract EC-77-S-02-4506 and LBL Subcontract 4503110. Thanks are due to Dr. I. D. Raistrick of Stanford, and Dr. W. Weppner and Professor H. G. von Schnering of Stuttgart for valuable discussions concerning the interpretation of these results.

References

1. N. P. YAO, L. A. HEREDY, AND R. C. SAUNDERS, *J. Electrochem. Soc.* **118,** 1039 (1971).
2. E. C. GAY, D. R. VISSERS, F. J. MARTINO, AND K. E. ANDERSON, *J. Electrochem. Soc.* **123,** 1591 (1976).
3. S. C. LAI, *J. Electrochem. Soc.* **123,** 1196 (1976).
4. R. A. SHARMA AND R. N. SEEFURTH, *J. Electrochem. Soc.* **123,** 1763 (1976).
5. R. N. SEEFURTH AND R. A. SHARMA, *J. Electrochem. Soc.* **124,** 1207 (1977).
6. R. P. ELLIOTT, "Constitution of Binary Alloys," 1st suppl., p. 586, McGraw-Hill, New York (1965).
7. F. A. SHUNK, "Constitution of Binary Alloys," 2nd suppl., p. 480, McGraw-Hill, New York (1969).
8. H. AXEL, H. SCHAFER, AND A. WEISS, *Angew. Chem.* **77,** 379 (1965).
9. H. SCHAFER, H. AXEL, AND A. WEISS, *Z. Naturforsch. B* **20,** 1302 (1965).
10. U. FRANK, W. MULLER, AND H. SCHAFER, *Z. Naturforsch. B* **30,** 10 (1975).
11. H. SCHAFER, H. AXEL, E. MENGES, AND A. WEISS, *Z. Naturforsch. B* **20,** 394 (1965).
12. H. SCHAFER, H. AXEL, AND A. WEISS, *Z. Naturforsch. B* **20,** 1010 (1965).
13. W. KLEMM AND M. STRUCK, *Z. Anorg. Chem.* **278,** 117 (1955).
14. V. H. BOHM, *Z. Metallk.* **50,** 44 (1959).
15. E. I. GLADYSHEVSKII, G. I. OLEKSIV, AND P. I. KRIPYAKEVICH, *Kristallografiya* **9,** 338 (1964); *Sov. Phys. Crystallogr.* **9,** 269 (1964).
16. H. AXEL, H. SCHAFER, AND A. WEISS, *Z. Naturforsch. B* **21,** 115 (1966).
17. H. G. VON SCHNERING, R. NESPER, K.-F. TEBBE, AND J. CURDA, Unpublished results (1980).
18. H. G. VON SCHNERING, R. NESPER, K.-F. TEBBE, AND J. CURDA, *Z. Metallk.* **71,** 357 (1980).
19. U. FRANK, W. MULLER, AND H. SCHAFER, *Z. Naturforsch. B* **30,** 1 (1975).
20. L. R. MCCOY AND S. LAI, *in* "Proceedings of the Symposium and Workshop on Advanced Battery Research and Design," p. B-167, U.S. ERDA Report No. ANL-76-8, March, 1976.
21. S.-C. LAI, *J. Electrochem. Soc.* **123,** 1196 (1976).
22. C. J. WEN, Ph.D. Dissertation, Stanford University (1980).
23. C. S. FULLER AND J. D. DITZENBERGER, *Phys. Rev.* **91,** 193 (1953).
24. J. C. SEVERIENS AND C. S. FULLER, *Phys. Rev.* **92,** 1322 (1953).
25. C. S. FULLER AND J. C. SEVERIENS, *Phys. Rev.* **96,** 21 (1954).
26. E. M. PELL, *Phys. Rev.* **119,** 1014; **119,** 1222 (1960).
27. B. PRATT AND F. FRIEDMAN, *J. Appl. Phys.* **37,** 1893 (1966).
28. L. G. YUSKESHIEVA AND A. S. ANTONOV, *Sov. Phys. Solid State* **8,** 2025 (1967).
29. J. C. LARUE, *Phys. Status Solidi A* **6,** 143 (1971).
30. W. WEPPNER AND R. A. HUGGINS, *J. Electrochem. Soc.* **124,** 1569 (1977).
31. W. WEPPNER AND R. A. HUGGINS, *J. Electrochem. Soc.* **125,** 7 (1978).
32. C. J. WEN, W. WEPPNER, B. A. BOUKAMP, AND R. A. HUGGINS, *J. Electrochem. Soc.* **126,** 2258 (1979).
33. C. J. WEN, W. WEPPNER, B. A. BOUKAMP, AND R. A. HUGGINS, *Metal. Trans. B* **11,** 131 (1980).
34. C. J. WEN, C. HO, B. A. BOUKAMP, I. D. RAISTRICK, W. WEPPNER, AND R. A. HUGGINS, *Inernat. Metals Rev.*, to be published.
35. C. WAGNER, *in* "Progress in Solid State Chemistry" (H. Reiss and J. D. McCaldin, Eds.), Vol. 6, p. 1, Pergamon, New York (1971).
36. E. M. PELL, *Phys. Chem. Solids* **3,** 77 (1957).
37. C. S. FULLER AND H. REISS, *J. Chem. Phys.* **27,** 318 (1957).